

Head-to-Head Comparison of ^{68}Ga -NOTA (^{68}Ga -NGUL) and ^{68}Ga -PSMA-11 in Patients with Metastatic Prostate Cancer: A Prospective Study

Minseok Suh^{1,2}, Hyung-Jun Im^{2,3}, Hyun Gee Ryoo^{1,2}, Keon Wook Kang¹, Jae Min Jeong¹, Sneha Prakash⁴, Sanjana Ballal⁴, Madhav P. Yadav⁴, Chandrasekhar Bal⁴, Chang Wook Jeong⁵, Cheol Kwak⁵, and Gi Jeong Cheon^{1,6,7}

¹Department of Nuclear Medicine, Seoul National University College of Medicine, Seoul, Korea; ²Department of Molecular Medicine and Biopharmaceutical Sciences, Graduate School of Convergence Science and Technology, Seoul National University, Seoul, Korea; ³Department of Applied Bioengineering, Graduate School of Convergence Science and Technology, Seoul National University, Seoul, Korea; ⁴Department of Nuclear Medicine, AIIMS, New Delhi, India; ⁵Department of Urology, Seoul National University College of Medicine, Seoul, Korea; ⁶Cancer Research Institute, Seoul National University, Seoul, Korea; and ⁷Institute of Radiation Medicine, College of Medicine, Seoul National University, Seoul, Korea

^{68}Ga -NOTA Glu-Urea-Lys (NGUL) is a novel prostate-specific membrane antigen (PSMA)-targeting tracer used for PET/CT imaging. This study aimed to compare performance in the detection of primary and metastatic lesions and to compare biodistribution between ^{68}Ga -NGUL and ^{68}Ga -PSMA-11 in the same patients with prostate cancer.

Methods: Eleven patients with metastatic prostate cancer were prospectively recruited. The quantitative tracer uptake was determined in normal organs and in primary and metastatic lesions. **Results:** ^{68}Ga -NGUL showed significantly lower normal-organ uptake and rapid urinary clearance. The number and sites of detected PSMA-positive primary and metastatic lesions were identical, and no significant quantitative uptake difference was observed. ^{68}Ga -NGUL showed a relatively lower tumor-to-background ratio than ^{68}Ga -PSMA-11. **Conclusion:** In a head-to-head comparison with ^{68}Ga -PSMA-11, ^{68}Ga -NGUL showed lower uptake in normal organs and similar performance in detecting PSMA-avid primary and metastatic lesions. ^{68}Ga -NGUL could be a valuable option for PSMA imaging.

Key Words: prostate-specific membrane antigen; ^{68}Ga -NGUL; ^{68}Ga -PSMA-11; biodistribution

J Nucl Med 2021; 62:1457–1460

DOI: 10.2967/jnumed.120.258434

Prostate-specific membrane antigen (PSMA), a transmembrane protein overexpressed in prostate cancer, has been one of the most highlighted targets for imaging and therapy of prostate cancer (1,2). Among many PSMA PET tracers, ^{68}Ga -PSMA-11 is the most extensively investigated and well-established tracer (3). ^{68}Ga -PSMA-11 is superior to conventional imaging modalities in staging and detection of biochemical failure in patients with prostate cancer (4–7).

We recently developed a novel PSMA-targeting tracer named ^{68}Ga -NOTA-Glu-Urea-Lys (NGUL), based on Glu-Urea-Lys

derivatives conjugated with NOTA chelator via a thiourea-type short linker (8). In our previous study, ^{68}Ga -NGUL showed a higher tumor-to-background ratio and substantially lower kidney uptake than ^{68}Ga -PSMA-11 in PSMA-positive tumor-xenografted mice (8).

To further investigate the clinical feasibility of ^{68}Ga -NGUL, we have conducted a prospective head-to-head comparison study between ^{68}Ga -NGUL and ^{68}Ga -PSMA-11 PET/CT. The specific aims of this study were to compare the detection efficacy and biodistribution between ^{68}Ga -NGUL and ^{68}Ga -PSMA-11 in the same patients with metastatic prostate cancer.

MATERIALS AND METHODS

Subjects

Patients with metastatic prostate cancer were prospectively recruited into this study. Each patient underwent ^{68}Ga -NGUL and ^{68}Ga -PSMA-11 PET/CT. The quality of the tracer was assessed before administration, and ^{68}Ga -NGUL showed high purity and stability (Supplemental Fig. 1; supplemental materials are available at <http://jnm.snmjournals.org>). This study was approved by the Institutional Review Board. All patients gave written informed consent to undergo 2 consecutive PSMA-targeted PET/CT scans. All procedures performed in this study were in accordance with the ethical standards of the institutional research committee and with the 1964 Helsinki declaration and its later amendments or comparable ethical standards.

Image Acquisition and Analysis

The PET/CT scans were obtained at 60 min after tracer injection. Any focal accumulation of ^{68}Ga -NGUL and ^{68}Ga -PSMA-11 not explained by physiologic uptake was defined as a pathologic lesion. Lesion numbers and lesion uptake, as SUV_{max} , were compared (Supplemental Fig. 2A). Tracer uptake was quantified in normal organs, including salivary glands, liver, spleen, and kidney, and blood-pool activity was measured in the inferior vena cava (Supplemental Fig. 2B). The normal-organ distribution of both tracers was quantified as SUV_{mean} . In addition, 3 patients underwent dynamic PET/CT scanning (60 min) of the pelvic region to evaluate the urinary clearance.

Statistical Analysis

Statistical analyses were performed using Prism, version 5.0 (GraphPad Software), and the MedCalc statistical packages, version 14.8 (MedCalc Statistical Software). Shapiro–Wilk testing was used to

Received Oct. 20, 2020; revision accepted Jan. 28, 2021.

For correspondence or reprints, contact Gi Jeong Cheon (larrycheon@gmail.com).

Published online February 26, 2021.

COPYRIGHT © 2021 by the Society of Nuclear Medicine and Molecular Imaging.

evaluate data normality. The 2 tracers were compared using the Wilcoxon signed-rank test, linear regression, and Bland–Altman analysis.

RESULTS

Eleven patients were prospectively enrolled into the study. Their characteristics are summarized in Supplemental Table 1. The interval between ^{68}Ga -NGUL and ^{68}Ga -PSMA-11 PET/CT was 1–4 d, and no patient received any treatment between the scans. Quantitative data are expressed as the median and interquartile range (IQR).

Normal-Organ Distribution

Overall, the 2 scans showed similar distribution patterns, with the highest uptake in the kidneys (Fig. 1). An intrapatient quantitative comparison revealed significant differences in organ uptake

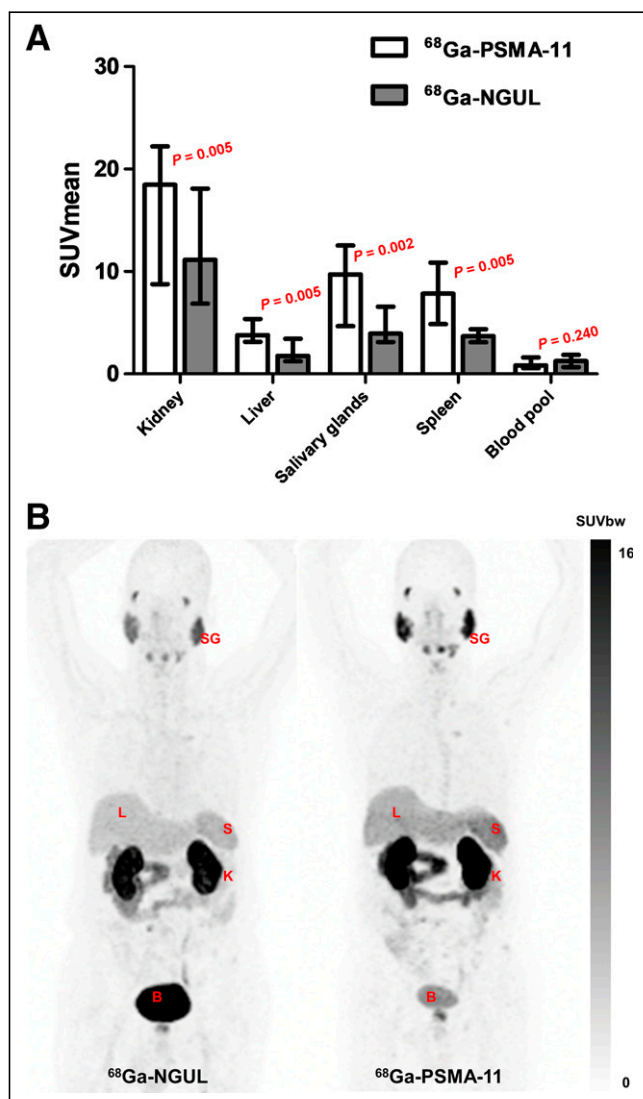


FIGURE 1. (A) SUV_{mean} of normal organs for ^{68}Ga -PSMA-11 and ^{68}Ga -NGUL. Median with interquartile range as error bar is plotted on bar chart. Wilcoxon signed-rank test for paired data was used for statistical comparison. (B) Representative image showing normal-organ distribution of ^{68}Ga -PSMA-11 and ^{68}Ga -NGUL. B = bladder; K = kidney; L = liver; S = spleen; SG = salivary glands; SUV_{bw} = SUV body weight.

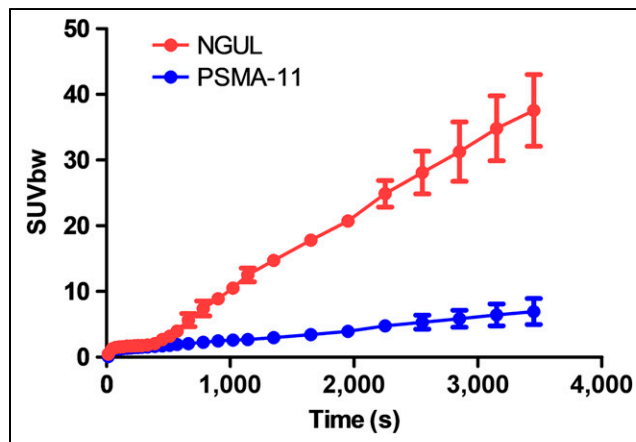


FIGURE 2. Time-activity curve of both ^{68}Ga -PSMA-11 and ^{68}Ga -NGUL derived from bladder region of interest.

between the 2 scans. The SUV_{mean} in the kidneys, salivary glands, spleen, and liver was significantly lower for ^{68}Ga -NGUL than for ^{68}Ga -PSMA-11 (Supplemental Table 2; Fig. 1). Linear correlation and agreement between ^{68}Ga -NGUL and ^{68}Ga -PSMA-11 are demonstrated in Supplemental Table 2 and Supplemental Fig. 3.

From the dynamic PET imaging, the time-activity curve of the bladder was obtained for both tracers (Fig. 2). Over time, higher bladder retention was observed for ^{68}Ga -NGUL, reflecting more rapid urinary clearance than for ^{68}Ga -PSMA-11.

Analysis of Primary and Metastatic Lesions

^{68}Ga -NGUL and ^{68}Ga -PSMA-11 could detect primary lesions in all patients ($n = 11$). There was no significant difference in the SUV_{max} of primary tumors (Fig. 3A; Supplemental Table 2).

In a total of 11 patients, 161 nodal and 59 bone PSMA-avid metastases were identified. All lesions were detected identically by both tracers, and none of the lesions was detected by only ^{68}Ga -NGUL or only ^{68}Ga -PSMA-11 (Supplemental Table 3). Quantitative uptake was evaluated in a total of 36 lesions (20 lymph nodes and 16 bone metastases); a maximum of 2 lesions per organ and a total of 5 lesions were selected in each patient. No significant differences in lymph node or bone metastasis uptake were observed between ^{68}Ga -NGUL and ^{68}Ga -PSMA-11 (Fig. 3A; Supplemental Table 2). Linear correlation and agreement between ^{68}Ga -NGUL and ^{68}Ga -PSMA-11 are demonstrated in Supplemental Table 2 and Supplemental Fig. 4. The median tumor-to-background ratio of ^{68}Ga -NGUL tended to be lower than that of ^{68}Ga -PSMA-11 in primary tumors (37.5 [IQR, 26.8–62.8] vs. 58.3 [IQR, 33.5–90.4]; $P = 0.067$) and lymph node metastases (29.7 [IQR, 18.5–55.9] vs. 48.1 [IQR, 12.5–99.1]; $P = 0.114$), and the difference was statistically significant in the case of bone metastases (48.7 [IQR, 29.1–61.9] vs. 81.0 [IQR, 25.7–97.8]; $P = 0.007$) (Fig. 3B).

DISCUSSION

We found that ^{68}Ga -NGUL showed lower uptake in the normal organs, including the kidneys, salivary glands, spleen, and liver. ^{68}Ga -NGUL also showed more rapid clearance through the urinary system than did ^{68}Ga -PSMA-11. There was no significant difference in absolute lesion uptake; however, tumor-to-background ratio tended to be lower for ^{68}Ga -NGUL than for ^{68}Ga -PSMA-11.

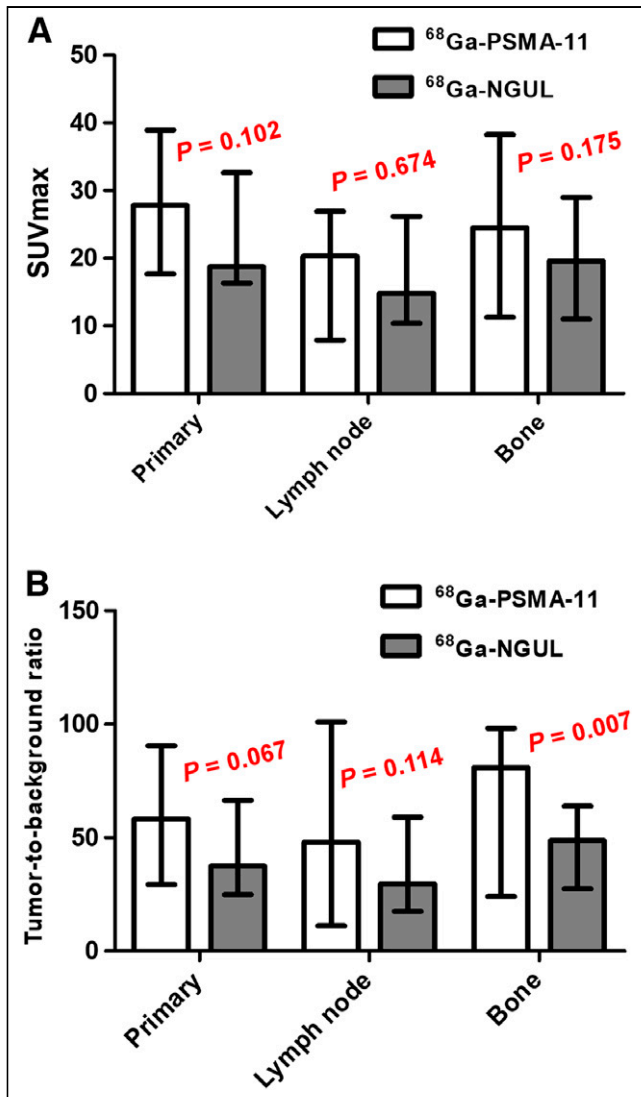


FIGURE 3. (A) SUV_{max} of primary tumor, lymph node, and bone metastases for ^{68}Ga -PSMA-11 and ^{68}Ga -NGUL. (B) Tumor-to-background ratio of primary tumor, lymph node, and bone metastases for ^{68}Ga -PSMA-11 and ^{68}Ga -NGUL. Median with interquartile range as error bar is plotted on bar chart. Wilcoxon signed-rank test for paired data was used for statistical comparison.

Still, the ability to detect primary and metastatic lesions was identical between ^{68}Ga -NGUL and ^{68}Ga -PSMA-11.

Several biodistribution studies of ^{68}Ga -PSMA-11 have demonstrated well the cellular expression of PSMA throughout the body: in parts of the lacrimal glands and major salivary glands, liver, spleen, kidneys, and intestines (9,10). In this study, ^{68}Ga -NGUL showed a distribution pattern visually similar to that of ^{68}Ga -PSMA-11. However, clearance via the urinary tract was more rapid for ^{68}Ga -NGUL than for ^{68}Ga -PSMA-11. Also, normal-organ uptake of ^{68}Ga -NGUL in the kidney, liver, salivary glands, and spleen was significantly lower than that of ^{68}Ga -PSMA-11. Several factors, including hydrophilicity, small molecular size, and low protein-binding properties, could explain the rapid clearance of ^{68}Ga -NGUL (11,12). NGUL has a lower molecular weight (769.82 vs. 947 g/mol) and higher hydrophilicity (log P = -3.3 vs. -3.9)

than PSMA-11 (Supplemental Fig. 5). Indeed, as a diagnostic imaging agent, ^{68}Ga -NGUL may interfere with the detection of lesions adjacent to the urinary tract because of early clearance through the kidney to the bladder. To overcome this limitation, proper hydration and a postvoiding delayed scan should be considered in future imaging protocols for ^{68}Ga -NGUL.

Despite the faster clearance of ^{68}Ga -NGUL, there was a trend toward a lower tumor-to-background ratio. In our previous study, the binding affinity of ^{68}Ga -NGUL was 18.3 nM (8), which is relatively lower than that of ^{68}Ga -PSMA-11, reported to be 24.3 nM (13). Thus, it is speculated that the fraction of unbound ^{68}Ga -NGUL is relatively higher than that of ^{68}Ga -PSMA-11 and the amount taken up by normal organs or tumor is relatively lower. As a result, the difference in the tumor-to-background ratio becomes more pronounced.

Some limitations should be noted. First, because of a small number of patients, we cannot draw a generalized conclusion. However, as a head-to-head comparison study, the difference between the distribution of the 2 compounds seems to be solid. Nonetheless, further studies with a larger number of patients are needed to validate our findings. Second, our cohort does not have whole-body PET data on multiple time points. As a result, we could not assess the clinical dose difference between the 2 agents. However, the effective dose measured from the animal experiments was 0.019 mSv/MBq (Supplemental Table 4), which is similar to the dosimetry data provided by ^{68}Ga PSMA-11 clinical studies. Lastly, the PSA level was not considered comprehensively. Because the PSMA-avid tumor burden correlates significantly with PSA level, it is considered to be a good indicator of tumor status at each scanning time point (4,14). However, since the interval between 2 scans was short, within 4 d, we speculate that the difference in tumor status between imaging time points is negligible.

CONCLUSION

A head-to-head comparison of ^{68}Ga -NGUL and ^{68}Ga -PSMA-11 revealed lower uptake of ^{68}Ga -NGUL in the normal organs, including the kidneys, salivary glands, spleen, and liver, and more rapid clearance through the urinary system. Although ^{68}Ga -NGUL showed a trend toward low tumor-to-background ratios, its ability to detect primary and metastatic lesions was the same as that of ^{68}Ga -PSMA-11. Therefore, ^{68}Ga -NGUL could be a valuable option for PSMA PET/CT imaging.

DISCLOSURE

This work was supported by a National Research Foundation of Korea grant funded by the Korean government (MSIT) (NRF-2020R1A2C2011428 and NRF-2020M2D9A1093988), by the Korea Health Technology R&D Project through the Korea Health Industry Development Institute (HI18C1916, HI19C0339), and by the Creative-Pioneering Researchers Program through Seoul National University. This work was supported by the Technology Innovation Program (20001235, Development of Novel Radiopharmaceutical for Prostate Cancer Targeted Imaging Diagnosis) funded by the Ministry of Trade, Industry, and Energy (Korea). The NGUL kit vial was provided by Cellbion Co., Ltd. Hyung-Jun Im, MD, PhD, is a consultant for Cellbion. No other potential conflict of interest relevant to this article was reported.

KEY POINTS

QUESTION: How does ^{68}Ga -NGUL PET/CT compare with ^{68}Ga -PSMA-11 in patients with metastatic prostate cancer?

PERTINENT FINDINGS: Compared with ^{68}Ga -PSMA-11, ^{68}Ga -NGUL showed lower uptake in the normal organs and more rapid clearance and tended to show a lower tumor-to-background ratio. Still, the ability to detect primary and metastatic lesions was identical between ^{68}Ga -NGUL and ^{68}Ga -PSMA-11, and no significant difference with respect to lesion uptake was observed.

IMPLICATIONS FOR PATIENT CARE: ^{68}Ga -NGUL can be a valuable option for imaging and theranostics in patients with metastatic prostate cancer.

REFERENCES

1. Irvani A, Violet J, Azad A, Hofman MS. Lutetium-177 prostate-specific membrane antigen (PSMA) theranostics: practical nuances and intricacies. *Prostate Cancer Prostatic Dis.* 2020;23:38–52.
2. Siva S, Udovicich C, Tran B, Zargar H, Murphy DG, Hofman MS. Expanding the role of small-molecule PSMA ligands beyond PET staging of prostate cancer. *Nat Rev Urol.* 2020;17:107–118.
3. Eder M, Schafer M, Bauder-Wust U, et al. ^{68}Ga -complex lipophilicity and the targeting property of a urea-based PSMA inhibitor for PET imaging. *Bioconjug Chem.* 2012;23:688–697.
4. Ceci F, Uprimny C, Nilica B, et al. ^{68}Ga -PSMA PET/CT for restaging recurrent prostate cancer: which factors are associated with PET/CT detection rate? *Eur J Nucl Med Mol Imaging.* 2015;42:1284–1294.
5. Fendler WP, Eiber M, Beheshti M, et al. ^{68}Ga -PSMA PET/CT: joint EANM and SNMMI procedure guideline for prostate cancer imaging: version 1.0. *Eur J Nucl Med Mol Imaging.* 2017;44:1014–1024.
6. Eiber M, Maurer T, Souvatzoglou M, et al. Evaluation of hybrid ^{68}Ga -PSMA ligand PET/CT in 248 patients with biochemical recurrence after radical prostatectomy. *J Nucl Med.* 2015;56:668–674.
7. Hofman MS, Lawrentschuk N, Francis RJ, et al. Prostate-specific membrane antigen PET-CT in patients with high-risk prostate cancer before curative-intent surgery or radiotherapy (proPSMA): a prospective, randomised, multicentre study. *Lancet.* 2020;395:1208–1216.
8. Moon SH, Hong MK, Kim YJ, et al. Development of a Ga-68 labeled PET tracer with short linker for prostate-specific membrane antigen (PSMA) targeting. *Bioorg Med Chem.* 2018;26:2501–2507.
9. Afshar-Oromieh A, Malcher A, Eder M, et al. PET imaging with a [^{68}Ga]gallium-labelled PSMA ligand for the diagnosis of prostate cancer: biodistribution in humans and first evaluation of tumour lesions. *Eur J Nucl Med Mol Imaging.* 2013;40:486–495.
10. Prasad V, Steffen IG, Diederichs G, Makowski MR, Wust P, Brenner W. Biodistribution of [^{68}Ga]PSMA-HBED-CC in patients with prostate cancer: characterization of uptake in normal organs and tumour lesions. *Mol Imaging Biol.* 2016;18:428–436.
11. Di L. Strategic approaches to optimizing peptide ADME properties. *AAPS J.* 2015;17:134–143.
12. Varma MV, Feng B, Obach RS, et al. Physicochemical determinants of human renal clearance. *J Med Chem.* 2009;52:4844–4852.
13. Kelly J, Amor-Coarasa A, Nikolopoulou A, et al. Synthesis and pre-clinical evaluation of a new class of high-affinity ^{18}F -labeled PSMA ligands for detection of prostate cancer by PET imaging. *Eur J Nucl Med Mol Imaging.* 2017;44:647–661.
14. Schmidkonz C, Cordes M, Schmidt D, et al. ^{68}Ga -PSMA-11 PET/CT-derived metabolic parameters for determination of whole-body tumor burden and treatment response in prostate cancer. *Eur J Nucl Med Mol Imaging.* 2018;45:1862–1872.